0022-3565/04/3081-143–155$20.00
THE JOURNAL OF PHARMACOLOGY AND EXPERIMENTAL THERAPEUTICS
Copyright © 2004 by The American Society for Pharmacology and Experimental Therapeutics
JPET 308:143–155, 2004

Vol. 308, No. 1
3282/1119306
Printed in U.S.A.

CYP3A4-Transfected Caco-2 Cells as a Tool for Understanding Biochemical Absorption Barriers: Studies with Sirolimus and Midazolam

Carolyn L. Cummins,[1] Wolfgang Jacobsen,[2] Uwe Christians,[3] and Leslie Z. Benet

Department of Biopharmaceutical Sciences, University of California San Francisco, San Francisco, California

Received August 6, 2003; accepted October 8, 2003

ABSTRACT

CYP3A4-transfected Caco-2 cells were used as an in vitro system to predict the importance of drug metabolism and transport on overall drug absorption. We examined the transport and metabolism of two drugs; midazolam, an anesthetic agent and CYP3A4 substrate, and sirolimus, an immunosuppressant and a dual CYP3A4/P-glycoprotein (P-gp) substrate, in the presence of cyclosporine (CsA, a CYP3A4/P-gp inhibitor) or *N*-{4-[2-(1,2,3,4-tetrahydro-6,7-dimethoxy-2-isoquinolinyl)-ethyl]-phenyl}-9,10-dihydro-5-methoxy-9-oxo-4-acridine carboxamine (GG918) (an inhibitor of P-gp and not CYP3A4). All major CYP3A4 metabolites were formed in the cells (1-OH > 4-OH midazolam and 39-*O*-desmethyl > 12-OH > 11-OH sirolimus), consistent with results from human liver microsomes. There was no bidirectional transport of midazolam across CYP3A4-transfected Caco-2 cells, whereas there was a 2.5-fold net efflux of sirolimus (1 μM) that disappeared in the presence of CsA or GG918. No change in the absorption rate or extraction ratio (ER) for midazolam was observed when P-gp was inhibited with GG918. Addition of GG918 had a modest impact on the absorption rate and ER for sirolimus (increased 58% and decreased 25%, respectively), whereas a 6.1-fold increase in the absorption rate and a 75% decrease in the ER were found when sirolimus was combined with CsA. Although both midazolam and sirolimus metabolites were preferentially excreted to the apical compartment, only sirolimus metabolites were transported by P-gp as determined from inhibition studies with GG918. Using CYP3A4-transfected Caco-2 cells we determined that, in contrast to P-gp, CYP3A4 is the major factor limiting sirolimus absorption. The integration of CYP3A4 and P-gp into a combined in vitro system was critical to unveil the relative importance of each biochemical barrier.

Oral bioavailability and intestinal drug absorption can be significantly limited by metabolizing enzymes and efflux transporters in the gut (Benet et al., 1996b). The most prevalent oxidative drug-metabolizing enzyme present in the intestine is cytochrome P450 3A4 (CYP3A4). Currently, more than 50% of the drugs on the market metabolized by P450 enzymes are metabolized by CYP3A4 (Benet et al., 1996a). Oral absorption of CYP3A4 substrates can also be limited by the multidrug resistance transporter P-glycoprotein (P-gp), because there is extensive substrate overlap between these two proteins (Wacher et al., 1995). P-gp is an ATP-dependent transporter on the apical plasma membrane of enterocytes that functions to limit the entry of drugs into the cell (Ambudkar et al., 1999). We have previously hypothesized that the interplay between CYP3A4 and P-gp in the intestine can serve to enhance drug metabolism and significantly decrease intestinal drug absorption (Cummins et al., 2002).

Human intestinal absorption of new drug candidates is frequently estimated by measuring the permeation of the drug across a monolayer of Caco-2 (colon carcinoma) cells (Artursson and Borchardt, 1997). For passively (and some

We gratefully acknowledge financial support provided by National Institutes of Health CA 72006 (to L.Z.B.) and Affymax Research Institute (to C.L.C.). L.Z.B. has a financial interest in and serves as Chairman of the Board of AvMax, Inc., a biotechnology company whose main interest is in increasing drug bioavailability by inhibiting intestinal CYP3A and P-glycoprotein. This work was presented in part as an oral presentation at the American Society for Pharmacology and Experimental Therapeutics Meeting in Orlando, FL, March 2001.

[1] Current address: Howard Hughes Medical Institute, University of Texas Southwestern Medical Center, Dallas, TX 75390.
[2] Current address: Biotechnology Centre of Oslo, University of Oslo, Oslo 0349, Norway.
[3] Current address: Department of Anesthesiology, University of Colorado Health Sciences Center, Denver, CO 80262. Article, publication date, and citation information can be found at http://jpet.aspetjournals.org.
DOI: 10.1124/jpet.103.058065.

ABBREVIATIONS: P-gp, P-glycoprotein; TPA, 12-*O*-tetradecanoylphorbol 13-acetate; MDR, multidrug resistance; MDCK, Madin-Darby canine kidney; CsA, cyclosporine; GG918, GF120918: *N*-{4-[2-(1,2,3,4-tetrahydro-6,7-dimethoxy-2-isoquinolinyl)-ethyl]-phenyl}-9,10-dihydro-5-methoxy-9-oxo-4-acridine carboxamine; PET, polyethylene terephthalate; HPLC, high-performance liquid chromatography; FBS, fetal bovine serum; TEER, transepithelial electrical resistance; LC/MS, liquid chromatography/mass spectrometry; M2, dihydrosirolimus; A, apical; B, basolateral; ER, extraction ratio; K77, K11777: *N*-methyl piperazine-Phe-homoPhe-vinylsulfone phenyl.

actively) transported compounds, the permeation rates obtained from this model have been shown to correlate with the percentage of drug absorbed (Artursson and Karlsson, 1991; Yee, 1997). Although Caco-2 cells express a variety of uptake and efflux transporters found in the human intestine, a major drawback to the use of Caco-2 cells is that they lack CYP3A4. As such, no data regarding the importance of intestinal metabolism on limiting drug absorption can be obtained from normal Caco-2 cells. Caco-2 cells pretreated with 1,25-dihydroxyvitamin-D_3 (vitamin D_3) express higher levels of CYP3A4 compared with Caco-2 (Schmiedlin-Ren et al., 1997) but still underestimate the amount of CYP3A4 in the human intestine (Paine et al., 2002). We have previously shown that the CYP3A4-transfected Caco-2 cells, when induced with both sodium butyrate and the phorbol ester 12-*O*-tetradecanoylphorbol 13-acetate (TPA), provide an appropriate in vitro model for studying intestinal drug transport and metabolism in intact cells as they have been found to closely approximate the CYP3A4 levels in human duodenum (Cummins et al., 2001).

In accordance with the hypothesized interplay between CYP3A4 and P-gp in the intestine, we have previously shown using CYP3A4-transfected Caco-2 cells that P-gp can enhance the metabolism of orally dosed drugs by repeated cycling of the drug at the apical membrane (Cummins et al., 2002). Here, we present transport and metabolism data for midazolam and sirolimus obtained in CYP3A4-transfected Caco-2 cells. These compounds were selected based on their distinct interactions with CYP3A4 and P-gp. Midazolam, a preoperative anesthetic agent, is a classic CYP3A4 substrate that has been shown to undergo extensive gut metabolism (Paine et al., 1996) and does not exhibit bidirectional transport by P-gp (Kim et al., 1999; Polli et al., 2001). The immunosuppressive drug sirolimus is a dual CYP3A4 and P-gp substrate that is known to be transformed by CYP3A4 to numerous hydroxylated and demethylated metabolites (Jacobsen et al., 2001) and has been shown to be an inhibitor of P-gp (Arceci et al., 1992). Conflicting evidence regarding its status as a P-gp substrate has emerged; some investigators have shown high net secretion (18-fold) (Crowe and Lemaire, 1998) and others have shown net absorption (Dias and Yatscoff, 1994; Wacher et al., 2002) across monolayers of Caco-2 cells. This discrepancy may reflect variability in transporter levels between different laboratories and various growth conditions tested. We confirmed the substrate selectivity of P-gp for sirolimus over midazolam using MDR1-transfected MDCK cells and examined the interplay of metabolism and transport in CYP3A4-transfected Caco-2 cells by using the inhibitors cyclosporine (CsA, inhibitor of CYP3A4 and P-gp) and GG918 (inhibitor of P-gp and not CYP3A4) in combination with each of the substrates.

The data obtained with CYP3A4-transfected Caco-2 cells demonstrate the variety of substrate-dependent complexities that can arise in the intestine and affect the determination of the intestinal extraction ratio. Sirolimus provides an especially interesting example because recent studies performed by Paine et al. (2002) using vitamin D_3-treated Caco-2 cells have suggested that a novel degradation pathway for sirolimus may play a more important role in intestinal extraction than metabolism by CYP3A4. In contrast, we have found using the CYP3A4-transfected Caco-2 cells that CYP3A4 metabolism seems more important than degradation at low sirolimus concentrations and that relative to CYP3A4, P-gp countertransport had little role in limiting sirolimus absorption across the cell. This study illustrates the importance of obtaining a cell culture model that accurately reflects the CYP3A4 content in the intestine when studying intestinal metabolism by CYP3A4.

Materials and Methods

Materials. Midazolam and 1-OH midazolam (F. Hoffman-La-Roche, Nutley, NJ), sirolimus (rapamycin, Rapamune; Wyeth-Ayerst, Princeton, NJ), and GG918 (GF120918; GlaxoSmithKline, Research Triangle Park, NC) were kind gifts of the manufacturers. Falcon polyethylene terephthalate (PET) cell culture inserts (diameter 4.2 cm^2) and Costar six-well plates were obtained from Fisher Scientific (Santa Clara, CA). Sodium butyrate, TPA, CsA, and ascomycin were purchased from Sigma-Aldrich (St. Louis, MO). All solvents were HPLC grade and were obtained from Fisher Scientific.

Cell Culture Growth Conditions. MDCK and MDR1-MDCK cells were generously provided by Dr. Ira Pastan (National Cancer Institute). Cells were grown in Dulbecco's modified Eagle's-H21 media supplemented with 10% fetal bovine serum (FBS) (HyClone Laboratories, Logan, UT) and 80 ng/ml colchicine for MDR1-MDCK cells. Cells were seeded at a density of 250,000 cells/insert, grown to confluence on PET inserts (diameter 4.2 cm^2), and maintained for 4 to 5 days before the experiment. Fresh media were added to the cells the day after seeding and 24 h before the transport study. CYP3A4-transfected Caco-2 cells (Gentest, Woburn, MA; passages 4 and 5) were grown using Dulbecco's modified Eagle's medium containing 8.5 g/l glucose, 25 mM HEPES, and 2.2 g/l $NaHCO_3$ and nonessential amino acids (custom made from the UCSF Cell Culture Facility, San Francisco, CA) containing 15% heat-inactivated FBS (HyClone Laboratories) and 100 μg/ml hygromycin B (Invitrogen, Carlsbad, CA). Cells were seeded onto PET cell culture inserts at a density of 300,000 cells/insert and grown to confluence for 13 to 14 days. Twenty-four hours before an experiment, the cell culture media were replaced with growth media containing 4 mM sodium butyrate and 100 nM TPA for CYP3A4 protein induction (Cummins et al., 2001).

Transport Studies across MDR1-MDCK and MDCK Cells. Cell monolayers were preincubated in transport buffer (Hanks' buffered salt solution containing 25 mM HEPES and 1% FBS, pH 7.4) for 30 min at 37°C. Transepithelial electrical resistance (TEER) values were measured across the monolayers using a Millicell (Millipore Corporation, Bedford, MA) equipped with chopstick electrodes. The average TEER values obtained for MDR1-MDCK and MDCK cells were 4830 ± 750 Ohm·cm^2 ($n = 12$) and 325 ± 14 Ohm·cm^2 ($n = 12$), respectively. The study was initiated by adding the test compound (midazolam or sirolimus) to the donor compartment and transport buffer to the receiver compartment. All solutions contained 1% dimethyl sulfoxide, and the final volume in each of the chambers was 1.5 ml on the apical side and 2.5 ml on the basolateral side. At the first two time points, 150-μl samples were taken from the receiver side and then replaced with fresh receiver solution to maintain the original starting volumes. After the last time point, the apical solutions were removed by suction, and each filter was dipped twice in three different beakers containing large volumes of ice-cold phosphate-buffered saline. The inserts were inverted to remove residual liquid, and intracellular measurements of parent drugs were obtained by solubilizing each cell culture insert with 1 ml of ice-cold MeOH/H_2O [7:3 (v/v)] and sonicating (in an ultrasonic bath) for 10 min. The homogenate was centrifuged for 5 min at 10,900*g*, and the resulting supernatant was analyzed by LC/MS.

Transport and Metabolism of Midazolam and Sirolimus across CYP3A4-Transfected Caco-2 Cells. The transport studies performed in CYP3A4-transfected Caco-2 cells were similar to those carried out using the MDR1-MDCK and MDCK cells except that metabolism was monitored along with transport. The TEER values

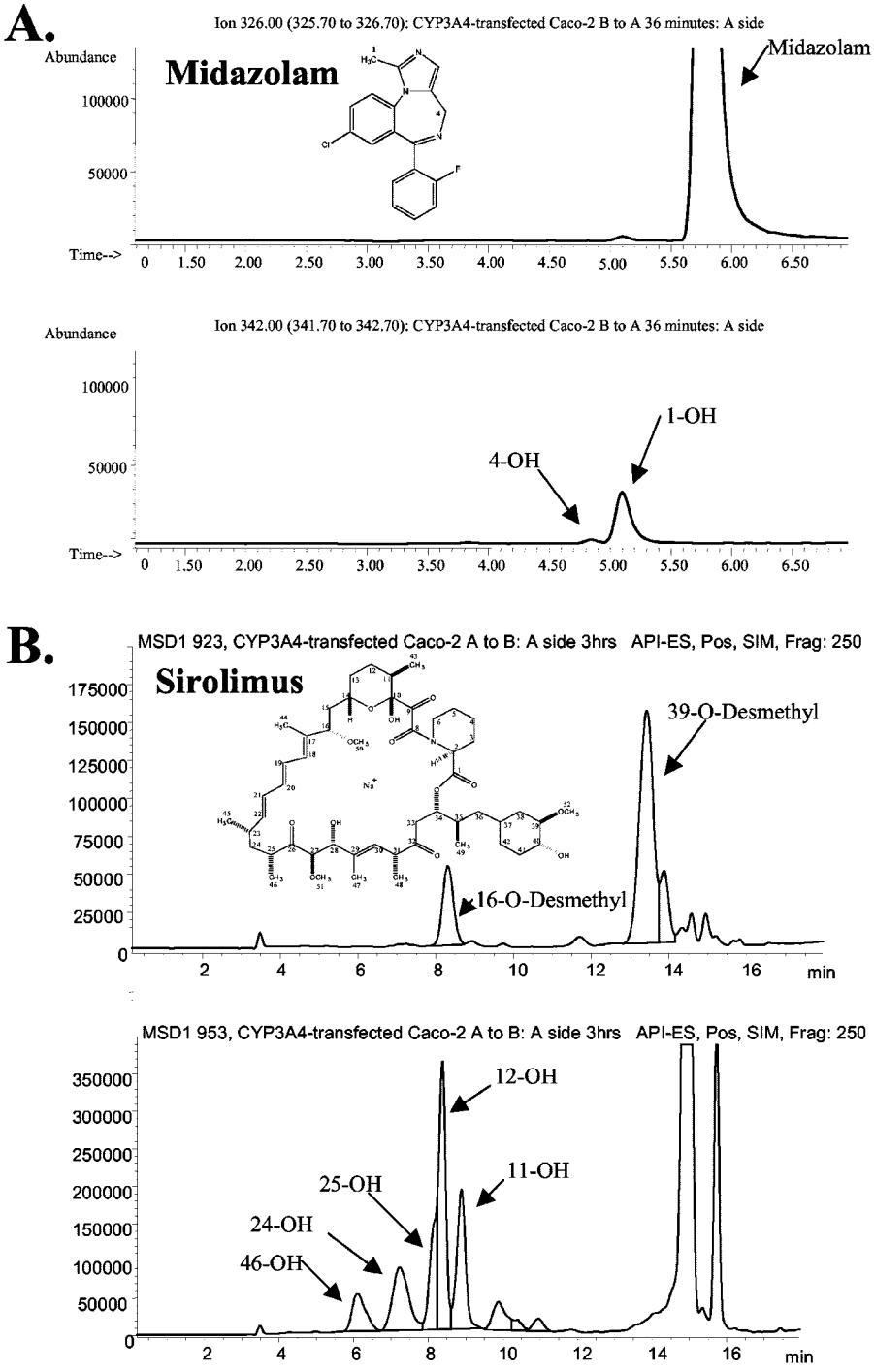

Fig. 1. A, LC/MS chromatograms of midazolam (m/z = 326) and its two hydroxylated metabolites (m/z = 342) found 36 min after incubation with CYP3A4-transfected Caco-2 cells from a 3 μM apical dose. B, LC/MS chromatograms of hydroxy-sirolimus ([M + Na], m/z 953) and the desmethyl-sirolimus metabolites ([M + Na], m/z 923) formed in CYP3A4-transfected Caco-2 cells 3 h after a 20 μM apical dose.

were measured after a 30-min preincubation of the cells in transport buffer. The average TEER value obtained for the CYP3A4-transfected Caco-2 cells was 334 ± 27 ohm·cm^2 (n = 84). In the experiments in which inhibitors were present, CsA (10 μM) or GG918 (200 nM), the same concentration of inhibitor was added to both sides of the monolayer. Because metabolism occurred inside the CYP3A4-transfected Caco-2 cells, samples were obtained from both sides of the monolayer at 12, 24, and 36 min (midazolam) or 1, 2, and 3 h (sirolimus). At the first two time points, 150-μl samples were taken from the receiver side and then replaced with fresh receiver solution to maintain the original starting volumes. The intracellular parent drug and metabolites were extracted as described above. Samples were stored at −80°C until analysis by LC/MS. Each experiment was conducted in triplicate on two separate occasions but due to slight interday cell variations, the data were analyzed separately from each experiment.

LC/MS Analysis of Midazolam, Sirolimus, and Their Metabolites. Midazolam transport and metabolite samples were analyzed by HPLC/electrospray-MS in combination with an on-line column switching extraction step using an HP1100 LC connected to a 5989B mass spectrometer through a 59987A electrospray interface (all Agilent Technologies, Palo Alto, CA). The solvents for the on-line column extraction step were delivered by a binary HPLC pump (PerkinElmer Instruments, Norwalk, CT) controlled by the external contacts of the HP1100 HPLC system. The sample was loaded onto the precolumn (Hypersil ODS, 2 × 10 mm, 10 μm; Keystone Scientific, Bellafonte, PA) with 2 mM ammonium acetate at 6 ml/min for 1 min and then backflushed onto the analytical column (4.6 × 50

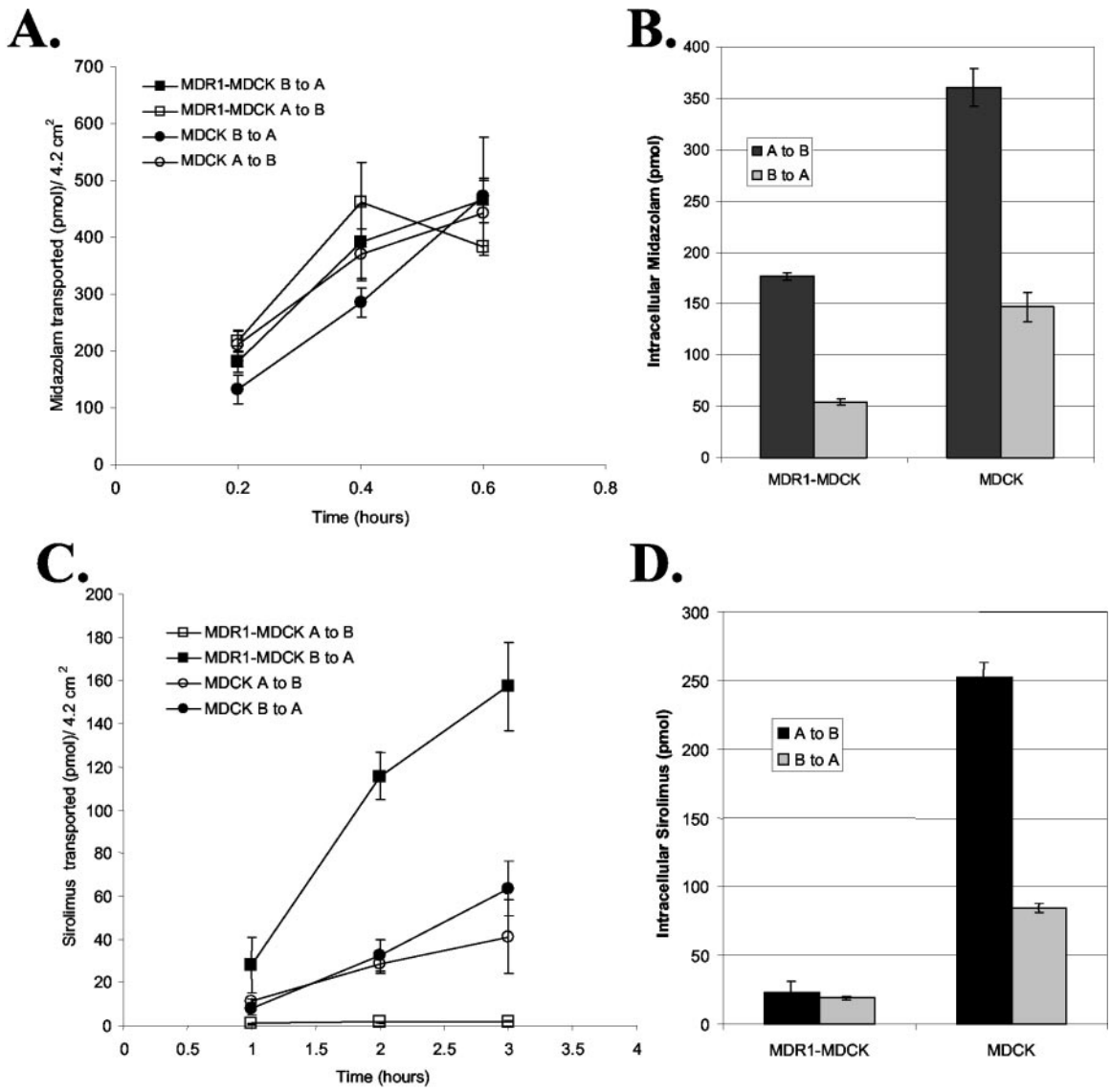

Fig. 2. Bidirectional transport of 3 μM midazolam (A) and 1 μM sirolimus (C) across MDR1-MDCK and MDCK cells. Intracellular levels of midazolam (B) and sirolimus (D) were measured in MDR1-MDCK and MDCK cells revealing the importance of P-gp in decreasing intracellular drug levels for P-gp substrates. Data shown represent the mean ± S.D. (n = 3).

mm, 3.5 μm) (Zorbax Eclipse XDB-C8; Agilent Technologies). The column temperature was maintained at 40°C, and the flow rate was 0.3 ml/min. The mobile phase consisted of 2 mM ammonium acetate and methanol. The following gradient was run: 0 min 70% methanol, 4 min 80% methanol. The total run time was 8 min. Using selective ion monitoring, signals for $[M + H]^+$ ions of midazolam (m/z = 326, retention time 5.8 min), 1-OH midazolam (m/z = 342, retention time 5.1 min), and 4-OH midazolam (m/z = 342, retention time 4.9 min) were obtained (Fig. 1A). Quantitation was performed using the external calibration curves for midazolam (2.5–320 ng/ml) and 1-OH midazolam (0.3–40 ng/ml).

Analysis of sirolimus and its metabolites was performed using an HPLC/electrospray-mass selective detector system in combination with an on-line column switching extraction step. The HPLC consisted of a quaternary pump (G1311A), degasser (G1322A), autosampler (G1329A) equipped with a thermostat (G1330A), and a column thermostat (G1316A) that was connected in series to a G1946A mass selective detector (all Agilent Technologies). Sirolimus and its metabolites were measured using a modification of a previously described method (Christians et al., 2000) to enhance the separation of the hydroxylated sirolimus metabolites. To 100 μl of sample, 50 μl of the internal standard solution (200 ng/ml ascomycin in acetonitrile) was added. Samples were loaded onto the precolumn (4.6 × 12.5 mm, 5 μm) (Eclipse XDB C8; Agilent Technologies) with 1 μM sodium acetate and 0.1% formic acid/methanol (68:32) at a rate of 5 ml/min for 0.8 min and then backflushed onto two analytical columns (4.6 × 150 mm, 3.5 μm) (Zorbax Eclipse XDB-C8; Agilent Technologies) positioned in series. The column temperature was maintained at 65°C, and the flow rate was 1.2 ml/min. The mobile phase consisted of 1 μM sodium acetate with 0.1% formic acid and methanol. The following gradient was run: 0 min 75% methanol, 10 min 75% methanol, 15 min 95% methanol. The total run time was 18.0 min. The most abundant ions observed for sirolimus and its metabolites were the sodium adducts. Using selective ion monitoring, signals for $[M + Na]^+$ ions of ascomycin (m/z = 815, retention time 12.5 min), sirolimus (m/z = 937, retention time 15.2 min), hydroxy-sirolimus (m/z = 953, retention times 6.2, 7.5, 8.4, 8.7, and 9.2 min for 46-OH, 24-OH, 25-OH, 12-OH, and 11-OH, respectively; Fig. 1B), demethylated sirolimus (m/z = 923, retention time 8.6 min for 16-O-desmethyl and 13.9 min for 39-O-desmethyl), seco-sirolimus (m/z = 937, retention time 15.6 min), and dihydrosirolimus (M2; m/z = 939, retention time 15.7 min) were observed. The structures and discussion of the latter

TABLE 1
Midazolam and sirolimus transport and inhibition across cell monolayers
Data shown are the average ± S.D. (n = 3).

Condition	$P_{app\ (A\rightarrow B)} \times 10^6$	$P_{app\ (B\rightarrow A)} \times 10^6$	Net Flux Ratio (B→A/A→B)
	cm/s		
Midazolam (3 μM)			
MDR1-MDCK cells	25 ± 4[a]	17 ± 1	0.7 ± 0.1
MDCK cells	16 ± 2	17 ± 4	1.1 ± 0.3
CYP3A4-transfected Caco-2	18.7 ± 0.9	18.1 ± 0.6	0.97 ± 0.06
+ CsA (10 μM)	21.0 ± 0.7*	19 ± 1	0.88 ± 0.07
+ GG918 (200 nM)	17 ± 1	18 ± 1	1.1 ± 0.1
Midazolam (10 μM)[b]			
CYP3A4-transfected Caco-2	16.5 ± 0.8	13.3 ± 0.9	0.81 ± 0.07
Sirolimus (1 μM)			
MDR1-MDCK cells	0.043 ± 0.008	3.5 ± 0.4	81 ± 17
MDCK cells	0.9 ± 0.4	1.4 ± 0.3	1.5 ± 0.7
CYP3A4-transfected Caco-2	0.29 ± 0.03	0.72 ± 0.03	2.5 ± 0.3
+ CsA (10 μM)	1.77 ± 0.06*	1.50 ± 0.04*	0.85 ± 0.04*
+ GG918 (200 nM)	0.45 ± 0.02*	0.36 ± 0.04*	0.8 ± 0.1*
Sirolimus (20 μM)			
CYP3A4-transfected Caco-2	1.7 ± 0.1	1.20 ± 0.02	0.70 ± 0.05

*$p < 0.05$ (relative to control treatment in that cell line).
[a] Permeability calculated up to 24 min instead of 36 min for this direction due to the nonlinearity beyond this point.
[b] Permeability calculated at 1 h for this experiment.

two compounds will be addressed subsequently (Fig. 7). The metabolite structures were identified as described previously (Jacobsen et al., 2001). Briefly, metabolites generated from human liver microsomes were isolated by HPLC, and structural identification was carried out by ion trap mass spectrometry and analysis of the fragmentation pattern. Because sufficient amounts of sirolimus metabolites were not available for a complete assay validation, the metabolite response factors were determined. Metabolites of sirolimus shared similar spectral characteristics as the parent drug, allowing the comparison of the peak area ratios for metabolite and parent from a single sample analyzed by UV to be compared with the same sample's metabolite to parent peak area ratios measured by MS. The metabolite MS response factors were very close to 1 (all metabolites deviated less than 15% from 1); therefore, the external calibration curve for sirolimus was used to quantitate its metabolites. The range of the standard curve for sirolimus was 0.3 to 160 ng/ml.

Despite attempts to accurately quantitate all known sirolimus metabolites and degradation products, we still obtained incomplete recovery after addition to CYP3A4-Caco-2 cells. The mass balance was directionally dependent with lower recovery from an apical dose (39–58%) compared with a basolateral dose (77–90%). This difference may be due to the presence of unidentified metabolites (formed predominantly after an apical dose) or nonspecific binding to the transport apparatus or cell surface.

Data Analysis. Calculation of the extraction ratio of midazolam was performed as described previously (Cummins et al., 2002). The extraction ratio is a measure of the extent of metabolism, that is, the fraction of drug that was metabolized relative to the amount of drug coming in contact with the enzyme. All values used in the calculation of the extraction ratio are in amounts. This extraction ratio incorporates in the denominator the intracellular amounts of unchanged drug, because it is reasoned that drug inside the cell can interact with CYP3A4.

$$ER = \frac{\Sigma\ \text{metabolites}_{(\text{donor+receiver+intracellular})}}{\Sigma\ \text{parent}_{(\text{receiver+intracellular})} + \Sigma\ \text{metabolites}_{(\text{donor+receiver+intracellular})}} \quad (1)$$

The permeability values were calculated as follows where the rate of transport was measured from the flux of drug across the cells (picomoles per hour):

$$P_{app} = \frac{\text{rate of transport}}{\text{surface area} \times \text{donor concentration}} \quad (2)$$

For comparing the treatment group (i.e., in the presence of inhibitors) with control, one-way analysis of variance followed by Dunnett's test was used to determine significance of data. For comparisons between two groups, the t test was used. The prior level of significance was set at $p < 0.05$.

Results

Transport of Midazolam and Sirolimus across MDR1-MDCK and MDCK Cells. Bidirectional transport studies across P-gp-overexpressing cells (MDR1-MDCK) and untransfected controls (MDCK) were performed to test the selectivity of P-gp for transporting sirolimus and midazolam. The transport of 3 μM midazolam in the apical (A) to basolateral (B) and B→A directions was similar in MDR1-MDCK and MDCK cells (Fig. 2A). These data confirm previous results obtained using L-MDR1 cells that showed midazolam was not a P-gp substrate (Kim et al., 1999). In contrast, there was a significant difference in the bidirectional transport of 1 μM sirolimus across MDR1-MDCK cells (Fig. 2C). The B→A flux was 80-fold greater than the A→B flux in MDR1-MDCK cells, and this efflux ratio decreased to 1.5 in MDCK cells, indicating that sirolimus was a good P-gp substrate (Table 1). Furthermore, the intracellular levels of sirolimus were significantly decreased in MDR1-MDCK relative to MDCK cells (Fig. 2D), indicating that P-gp was contributing to this phenomenon by actively effluxing the compound out of the cells. Intriguingly, the midazolam intracellular levels were also decreased in MDR1-MDCK cells (Fig. 2B), suggesting that some minor interaction with P-gp may be present in cells overexpressing P-gp, despite the lack of bidirectional midazolam transport across the cells. This idea is consistent with recent literature reports citing midazolam as a "nontransported P-gp substrate" (Polli et al., 2001) or a "highly permeable P-gp substrate" (Tolle-Sander et al., 2003). For both midazolam and sirolimus, the drug permeation was greater from the apical side, a result that could be due to greater surface area for permeation due to the apical microvilli.

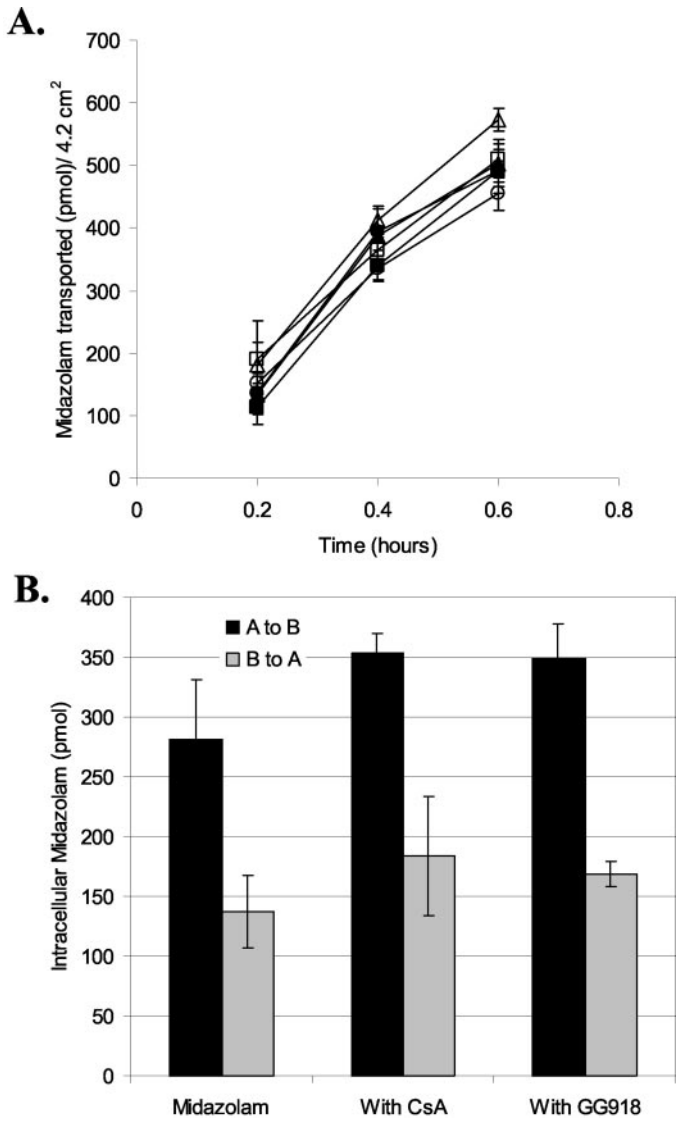

Fig. 3. A, transport of 3 μM midazolam (■, □) across CYP3A4-transfected Caco-2 cells in the presence of the P-gp inhibitors 10 μM CsA (▲, △) and 200 nM GG918 (●, ○). Basolateral to apical transport is represented with solid symbols and apical to basolateral is represented with open symbols. B, intracellular levels of midazolam after an apical or basolateral dose (measured at 36 min) in the presence of the inhibitors CsA and GG918. All data are presented as the mean ± S.D. (n = 3).

Midazolam Metabolism and Transport across CYP3A4-Transfected Caco-2 Cells. The concurrent transport and metabolism of midazolam was examined across monolayers of CYP3A4-transfected Caco-2 cells. The two primary midazolam metabolites, 1-OH midazolam and 4-OH midazolam, were readily observed after incubation with CYP3A4-transfected Caco-2 cells, and their LC/MS chromatograms are shown in Fig. 1A. Consistent with human data (Paine et al., 1996), 1-OH midazolam was the major metabolite formed and therefore 4-OH midazolam was not quantitated for these studies.

Midazolam transport (Fig. 3A) and permeability values (Table 1) were similar in both the A→B and B→A directions consistent with passive absorption. Due to the high permeation rate of midazolam, the transport studies were performed at relatively early time points (up to 36 min) to maintain sink conditions during the course of the experiment. Midazolam transport in both directions was unchanged in the presence of the P-gp inhibitor GG918. However, midazolam absorptive transport was increased 12% with CsA, suggesting metabolism by CYP3A4 is also affecting net midazolam absorption by decreasing substrate available for transport (Fig. 3A; Table 1). The results with GG918 confirm the lack of importance of P-gp in influencing midazolam transport. The intracellular levels of midazolam in CYP3A4-transfected Caco-2 cells further suggest no role for P-gp in controlling intracellular levels because there was no significant increase ($p > 0.05$) in the intracellular midazolam levels with P-gp inhibition (Fig. 3B).

Midazolam metabolism was found to be linear over the time course of the experiment. As midazolam is metabolized inside the cell, the excretion pattern of 1-OH midazolam was monitored by obtaining samples from both the apical and basolateral chambers at each time point. Intracellular 1-OH midazolam was also measured at the last time point to obtain an accurate total of the amount of metabolism that occurred. More midazolam metabolites were observed from an apical dose (Fig. 4, A versus B, y-axes) in agreement with the higher intracellular midazolam found from this direction (Fig. 3B). The proximity of CYP3A4 toward the apical membrane (Cummins et al., 2001) may also have increased metabolism from an apical dose because the experiment was run over a relatively short time period, and midazolam intracellular steady state has been shown previously to be achieved more rapidly from an apical dose (Fisher et al., 1999). There was preferential excretion of 1-OH midazolam to the apical side after administering an apical or basolateral dose of 3 μM midazolam (Fig. 4, A and B). The excretion of 1-OH midazolam was 7.7-fold greater out the apical side compared with the basolateral side (after an apical dose) and 5.6-fold greater out the apical side after a basolateral dose. These 1-OH midazolam efflux ratios were unchanged in the presence of the P-gp inhibitors GG918 and CsA, indicating that P-gp was not contributing to this phenomenon. There was no significant change in intracellular levels of 1-OH midazolam in the presence of GG918 (Fig. 4C), further indicating no interaction of P-gp. The metabolite levels were decreased with CsA, indicating CsA was directly inhibiting metabolism by CYP3A4.

Metabolism and Transport of Sirolimus across CYP3A4-Transfected Caco-2 Cells. The metabolism of sirolimus has been extensively characterized in human and intestinal microsomes as well as in cDNA-expressed cytochrome P450s (Lampen et al., 1998; Jacobsen et al., 2001). Sirolimus metabolism has been found to be mediated primarily by CYP3A4 with some contribution from CYP3A5 and CYP2C8 (Jacobsen et al., 2001). Five main hydroxylated and two main demethylated metabolites of sirolimus were found after incubation of 1 μM sirolimus with CYP3A4-transfected Caco-2 cells. The metabolite pattern from CYP3A4-transfected Caco-2 cells was consistent with that observed from human liver microsomes. The sirolimus metabolite LC/MS chromatograms are shown in Fig. 1B.

Sirolimus transport across CYP3A4-transfected Caco-2 cells was found to be 2.5-fold greater in the B→A direction compared with the A→B direction (Fig. 5A). The net efflux of

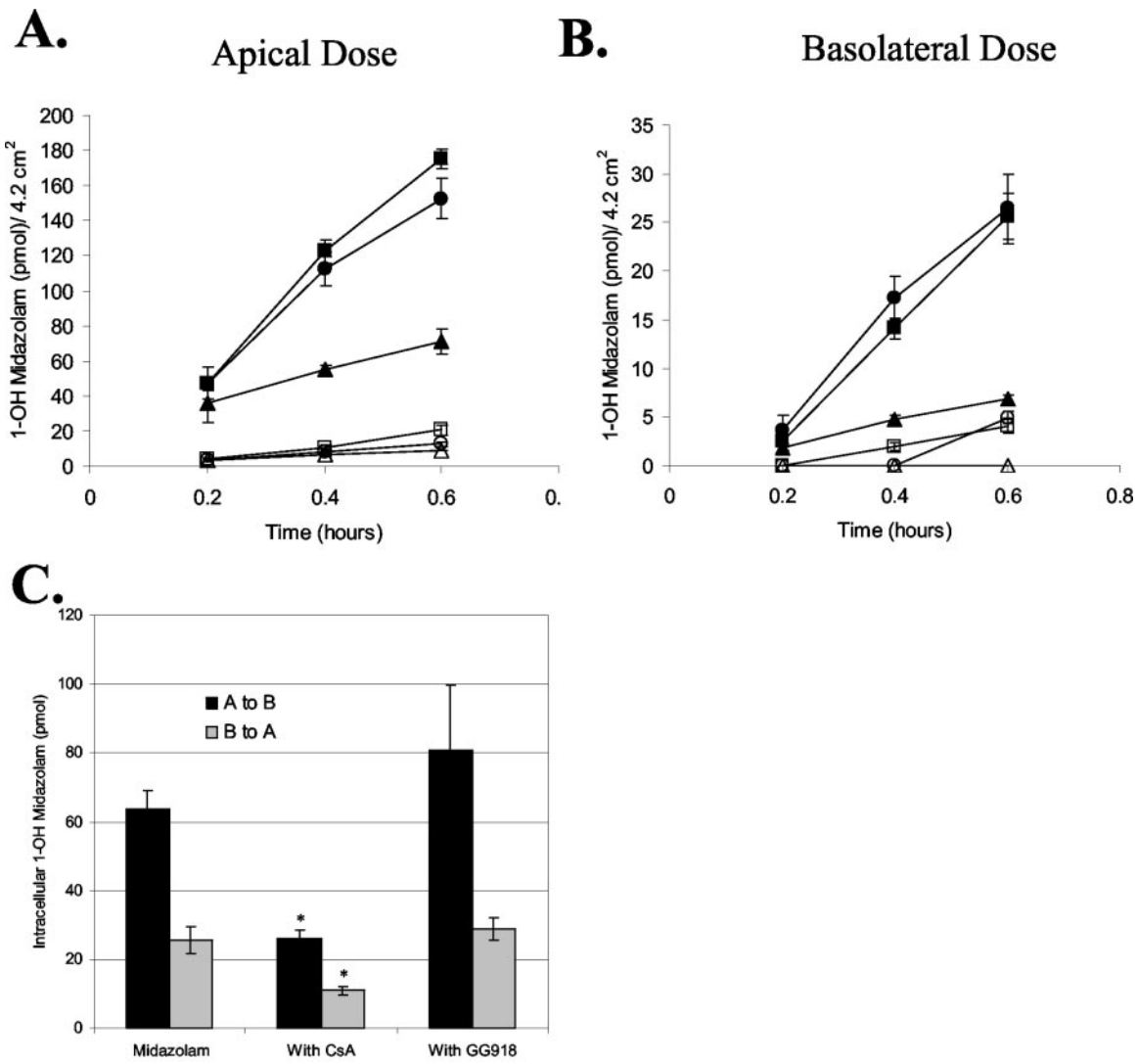

Fig. 4. 1-OH Midazolam exit profiles after a 3 μM midazolam apical (A) or basolateral (B) dose. Midazolam was dosed alone (■, □) or in combination with the inhibitors 10 μM CsA (▲, △) or 200 nM GG918 (●, ○). Metabolites were found exiting both the apical (solid symbols) and basolateral (open symbols) membranes. The 1-OH midazolam found inside the cells at 36 min after an apical or basolateral dose is shown in C. All data are presented as the mean ± S.D. (n = 3). *, significantly different from control value for that direction (A to B or B to A), $p < 0.05$.

1 μM sirolimus was completely inhibited in the presence of either 200 nM GG918 or 10 μM CsA, and the resulting transport profiles were found to be slightly inverted, that is, sirolimus A→B transport slightly exceeded that of B→A in the presence of the inhibitors. The efflux ratio was also less than 1 when sirolimus was dosed at 20 μM, indicating saturation of P-gp at this concentration (Table 1). The absorptive permeability of sirolimus increased 55% when P-gp was inhibited, but when both P-gp and CYP3A4 were inhibited it increased 6.1-fold (Table 1). The intracellular levels of sirolimus (Fig. 5B) after an apical dose were also affected more by CsA compared with GG918 where, respectively, a 3.8-fold increase versus a 31% increase was observed.

Sirolimus metabolite formation was shown to be generally linear with time (Fig. 6). The metabolites of sirolimus were preferentially excreted toward the apical side. The excretion patterns for the three main sirolimus metabolites (11-OH, 12-OH, and 39-O-desmethyl) are shown in Fig. 6. Significantly more metabolites were formed after an apical dose compared with a basolateral dose, as seen from the difference in the scales of the y-axes between the apical and basolateral doses (Fig. 6). The efflux ratios for metabolites (amount exiting apical/amount exiting basolateral) after an apical dose were 16, 28, and >14 for 11-OH, 12-OH, and 39-O-desmethyl, respectively. The efflux ratio for 39-*O*-desmethyl could not be explicitly calculated because the metabolite excretion from the basolateral side was below the limit of detection (0.1 ng/ml). In the presence of the P-gp inhibitors CsA and GG918, the metabolite efflux ratios (after an apical dose) were decreased more than 3-fold, resulting in efflux ratios between 4.0 and 5.5 for all three metabolites. The intracellular levels of metabolites were also increased in the presence of CsA and GG918, indicating that metabolite removal was inhibited. These data suggest the sirolimus metabolites are also substrates for P-gp transport. Although the amounts of intracellular sirolimus metabolites were increased in the presence of CsA, the total amounts of metabolites as measured in the apical and basolateral compartments were decreased 50%, presumably by the direct inhibition of CYP3A4 by CsA.

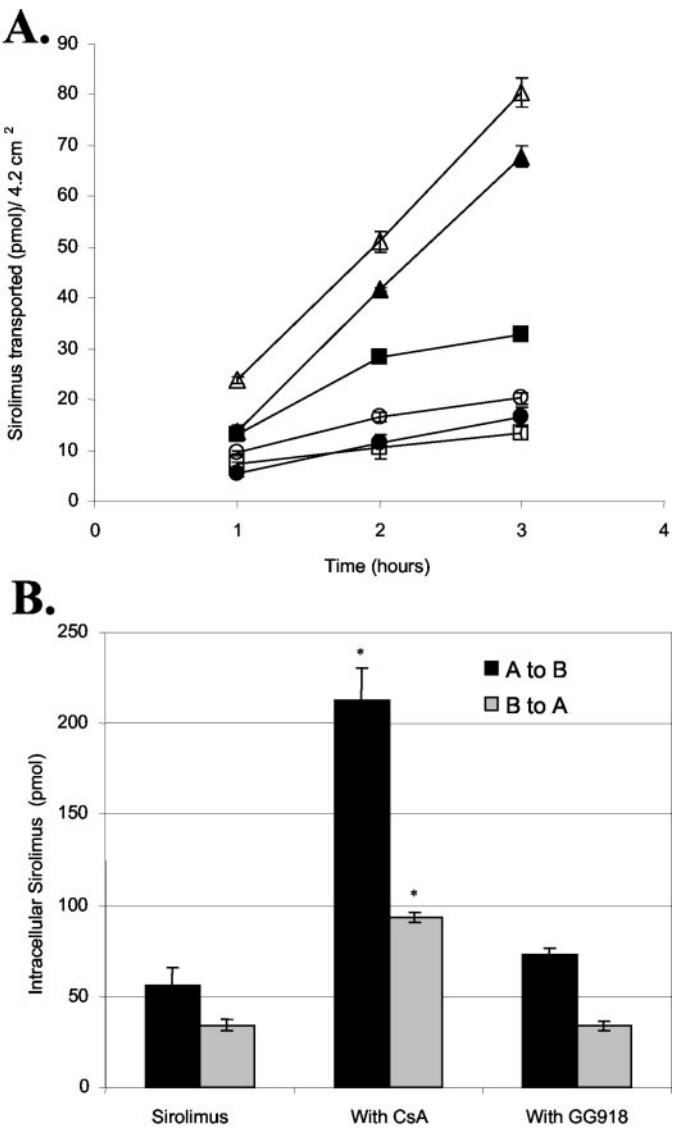

Fig. 5. A, bidirectional transport of 1 μM sirolimus (■, □) across CYP3A4-transfected Caco-2 cells in the presence of the P-gp inhibitors 10 μM CsA (▲, △) and 200 nM GG918 (●, ○). Basolateral to apical transport is represented with solid symbols and apical to basolateral is represented with open symbols. B, intracellular levels of sirolimus after an apical or basolateral dose (measured at 3 h) in the presence of the inhibitors CsA and GG918. All data are presented as the mean ± S.D. (n = 3). *, significantly different from control for that direction (A to B or B to A), $p < 0.05$.

Sirolimus Degradation Products in CYP3A4-Transfected Caco-2 Cells. Hallensleben et al. (2000) identified a novel metabolite of sirolimus (dihydrosirolimus) formed from the degradation of sirolimus to its ring opened isomer (seco-sirolimus) that then undergoes hydrogenation to form this new metabolite. The proposed metabolic pathway for the formation of dihydrosirolimus is shown in Fig. 7. It has recently been suggested that this degradation pathway to form M2 may be an important route of intestinal extraction from studies performed with 20 μM sirolimus in vitamin D_3-treated Caco-2 cells (Paine et al., 2002). In contrast, we discovered that in the CYP3A4-transfected Caco-2 cells that there was minimal conversion of sirolimus to seco-sirolimus after a 1 μM dose, and therefore only low levels of its metabolite dihydrosirolimus were found after 3 h of incubation. At a higher concentration of sirolimus (20 μM), seco-sirolimus and M2 were observed at earlier time points. However, there was nonlinearity in the amount of CYP3A4 metabolites formed at 20 μM (603 pmol) relative to 1 μM (105 pmol), indicating saturation of CYP3A4 at this concentration. Figure 8 shows the relative proportion of seco- and dihydrosirolimus plotted alongside the amount of CYP3A4 metabolites from 1 and 20 μM apical incubations. In our incubations, seco-sirolimus was always higher on the donor side, regardless of the direction of transport (Fig. 8, apical dose). When sirolimus was dosed basolaterally, seco-sirolimus was found mainly on the basolateral side, whereas the CYP3A4 metabolites were still excreted toward the apical side (data not shown). These results suggest that seco-sirolimus was likely formed from nonspecific degradation within the transport media. The amount of parent drug converted to seco-sirolimus after 3 h of incubation was approximately 1% of the dose at both concentrations tested.

All CYP3A4-derived sirolimus metabolites showed a similar distribution across the cell (>70% of metabolites found apical, ~20% basolateral, and <10% intracellular) with the exception of 39-*O*-desmethyl sirolimus that had a much greater metabolite fraction inside the cell (~40%; Fig. 8). The reason for the difference in the cellular distribution of 39-*O*-desmethyl is unknown because, as with the hydroxy metabolites, it was also found to be actively extruded by P-gp. It is possible that the increased cellular retention is due to stronger interactions with cellular proteins or related to its increased hydrophobicity, suggested by its longer retention on the reverse phase column. A similar trend was observed with seco-sirolimus and dihydrosirolimus at the 20 μM concentration.

Extraction Ratios of Midazolam and Sirolimus across CYP3A4-Transfected Caco-2 Cells. To obtain a measure of the extent of metabolism occurring upon transit across the CYP3A4-transfected Caco-2 monolayer, an ER was calculated using eq. 1. For sirolimus, only the known CYP3A4-generated metabolites were included in the calculation because the degradation of sirolimus to seco-sirolimus and dihydrosirolimus were minimal at the 1 μM concentration. The resulting ERs for midazolam and sirolimus in the presence of the inhibitors CsA and GG918 are shown in Fig. 9.

Consistent with midazolam not being a substrate for P-gp, the presence of GG918 did not alter the ER for midazolam in either direction. Cyclosporine decreased the ER for midazolam by 60% from both an apical and basolateral dose through inhibition of CYP3A4. An unexpected result was the difference in the ERs for midazolam from an apical and a basolateral dose (25 and 8%, respectively). In the absence of efflux transport, no difference in the apical and basolateral ERs was anticipated based on our previous findings with felodipine (another CYP3A4 substrate that is not transported by P-gp; Cummins et al., 2002). Although the calculation of the ER (eq. 1) takes into account the differences in the intracellular midazolam levels at the last time point, this equation assumes that the intracellular compartment reached equilibrium over a short time period relative to the time scale of the experiment. Fisher et al. (1999) have shown using vitamin D_3-induced Caco-2 cells that midazolam reaches steady state more slowly from a basolateral dose (>10 min) compared with an apical dose (3 min). The short time course for mida-

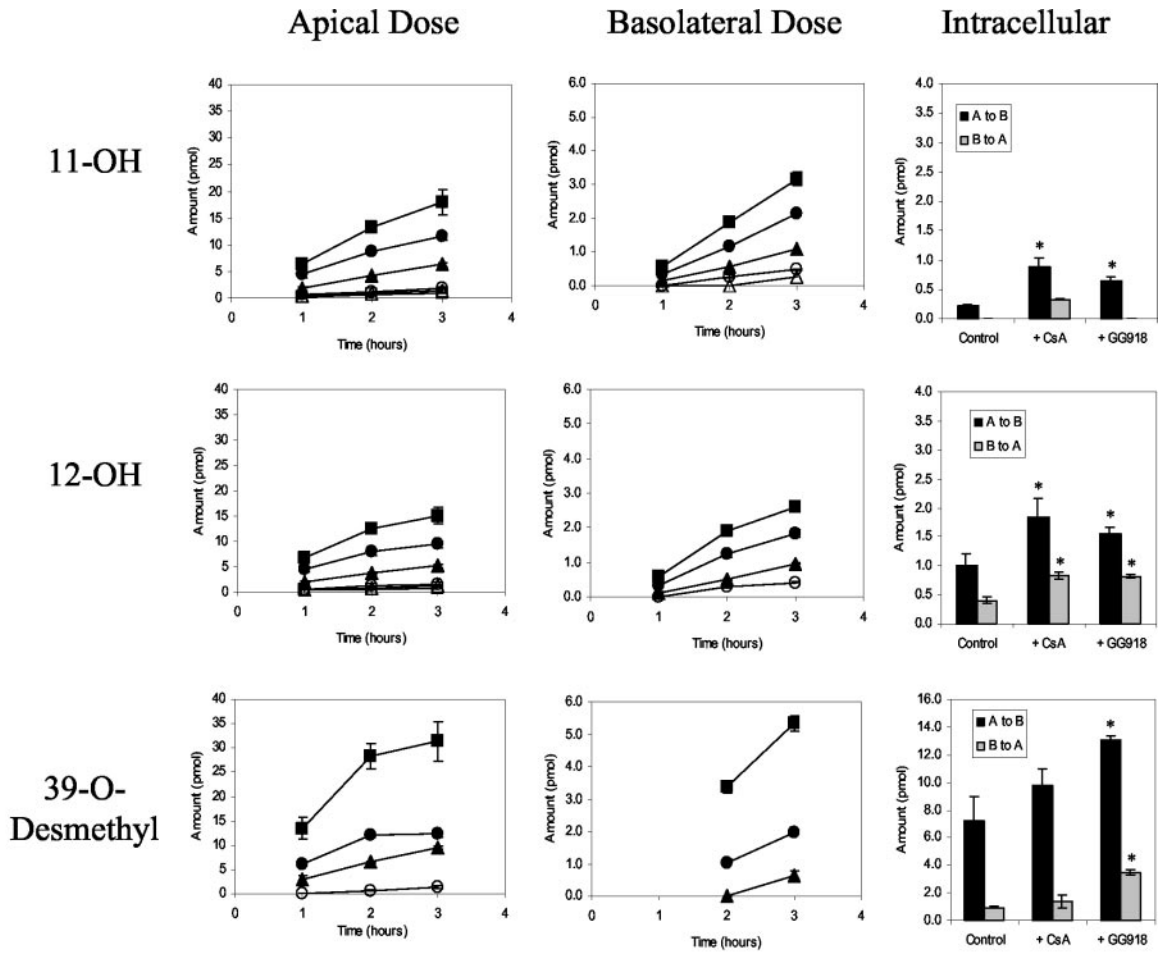

Fig. 6. Metabolite exit profiles for the three main sirolimus metabolites (11-OH, 12-OH, and 39-*O*-desmethyl-sirolimus) formed after 1 μM apical or basolateral dose in CYP3A4-transfected Caco-2 cells. Sirolimus was dosed alone (■, □) or in combination with the inhibitors 10 μM CsA (▲, △) or 200 nM GG918 (●, ○). Metabolites were found exiting both the apical (solid symbols) and basolateral (open symbols) membranes. Sirolimus metabolites found inside the cell after an apical or basolateral dose are plotted under the heading intracellular. The vertical axes for each direction were plotted on the same scale to allow comparison between metabolites. One exception is the intracellular vertical axis for 39-*O*-desmethyl that is 4 times higher than that of the hydroxylated metabolites. Only metabolite levels that were above the limit of detection were plotted. All data are presented as the mean ± S.D. (n = 3). *, significantly different from control for that direction (A to B or B to A), $p < 0.05$.

zolam may have resulted in an overestimation of the average intracellular amount of midazolam from a basolateral dose. This explanation is supported by a transport study that examined midazolam metabolism for a longer time period at 10 μM in which the ERs after 1.5 h became almost equal from each direction (23.5 ± 0.9 versus 18 ± 2%, apical versus basolateral; data not shown).

For sirolimus, the apical ER was decreased by 25% in the presence of the P-gp inhibitor GG918, demonstrating the moderate influence of P-gp in increasing the exposure of sirolimus to CYP3A4 after an apical dose (Fig. 9). From a basolateral dose, the ER increased by 17% with GG918, indicating the opposite role for P-gp in supporting drug removal from the cell after a basolateral dose. The presence of 10 μM cyclosporine greatly decreased the apical and basolateral sirolimus ERs (by 75%), indicating that CYP3A4 was significantly inhibited at this concentration.

Discussion

The functional utility of the CYP3A4-transfected Caco-2 cells for predicting the importance of various biochemical factors in limiting drug absorption was demonstrated in this study. Although transport studies can be performed in normal Caco-2 cells to determine whether a drug is a substrate for efflux transport, and intestinal microsomes can be used to calculate the expected intestinal intrinsic clearance, the relative importance of each of these individual factors in limiting overall drug absorption cannot easily be anticipated unless they are studied in combination. Our studies with midazolam and sirolimus have highlighted additional factors (i.e., intracellular equilibration time and interactions with multiple transporters) that add complexity to the calculation and interpretation of the extraction ratio. The sirolimus data support the dynamic interplay between P-gp and CYP3A4 in increasing intestinal metabolism that we reported previously (Cummins et al., 2002).

The ER for sirolimus (1 μM) after an apical dose decreased from 0.6 to 0.45 when P-gp alone was inhibited (with GG918). These data demonstrate that functional P-gp can enhance the extent of metabolism of sirolimus after an apical dose. The net efflux of sirolimus across CYP3A4-transfected cells became net absorptive transport when P-gp was saturated or after complete inhibition of P-gp with either CsA or GG918 (Table 1). The change in the net direction of transport sug-

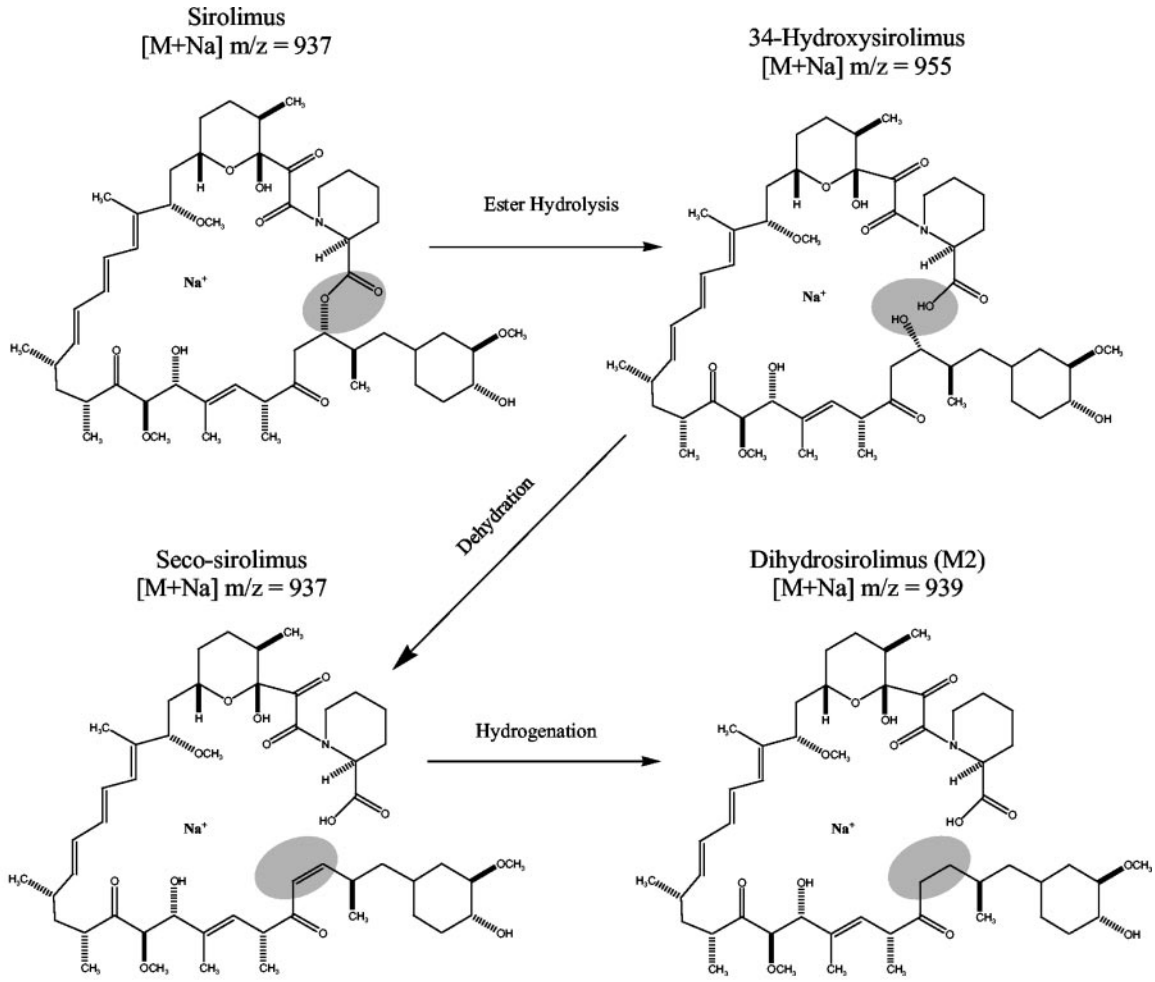

Fig. 7. Proposed pathway for the metabolic conversion of sirolimus to dihydrosirolimus (Hallensleben et al., 2000).

gests that sirolimus is also a substrate of an absorptive transporter that may be contributing to the difference in the apical versus basolateral extraction ratios that persisted after P-gp inhibition (Fig. 9). In contrast, there was no change in the ER for midazolam with GG918. There was a marked decrease in the sirolimus and midazolam apical ERs after coincubation with CsA due to direct inhibition of CYP3A4 by CsA. The absorption of midazolam occurred rapidly and therefore inhibition of CYP3A4 only resulted in a 12% increase in transcellular transport (Table 1). The difference in the apical and basolateral ERs for midazolam (0.25 versus 0.081) would not be anticipated considering that midazolam is not a substrate for efflux transport. This discrepancy may be due to a slower intracellular equilibration of midazolam from a basolateral dose (>10 min) versus an apical dose (3 min) as reported previously by Fisher et al. (1999). Because the midazolam transport experiment is run over 36 min, the basolateral intracellular value of midazolam obtained at the last time point is likely an overestimation of the average value of midazolam inside the cell over the course of the experiment, thereby resulting in an underestimation of the basolateral ER.

The metabolites of midazolam and sirolimus formed in the CYP3A4-transfected Caco-2 cells were preferentially excreted toward the apical side of the cell after either an apical or basolateral dose. The preference for the apical secretion of 1-OH midazolam was not altered in the presence of either GG918 or CsA, despite there being less metabolites formed with CsA. These data are in agreement with previous midazolam data obtained from vitamin D_3-treated Caco-2 cells where verapamil was unable to inhibit the preferential excretion of 1-OH midazolam toward the apical side (Schmiedlin-Ren et al., 1997). In contrast, the preference for the apical excretion of each of the three main sirolimus metabolites (11-OH, 12-OH, and 39-*O*-desmethyl) was significantly decreased in the presence of the P-gp inhibitors GG918 and CsA. These results suggest that P-gp was responsible for the extrusion of sirolimus metabolites from the cell. Together, these studies demonstrate the importance of inhibition studies to determine whether metabolites are substrates for efflux transport.

The concurrent study of metabolism and transport in CYP3A4-transfected Caco-2 cells permitted the characterization of the importance of each process in limiting overall sirolimus absorption. The net absorptive (A→B) flux of sirolimus was increased 6-fold when both CYP3A4 and P-gp were inhibited (CsA data), whereas it increased only 55% when P-gp alone was inhibited (GG918 data). The remarkable change in the absorptive permeability with CsA highlights the importance of CYP3A4 in this system in limiting drug absorption across the cell.

Paine et al. (2002) have reported the identification of a

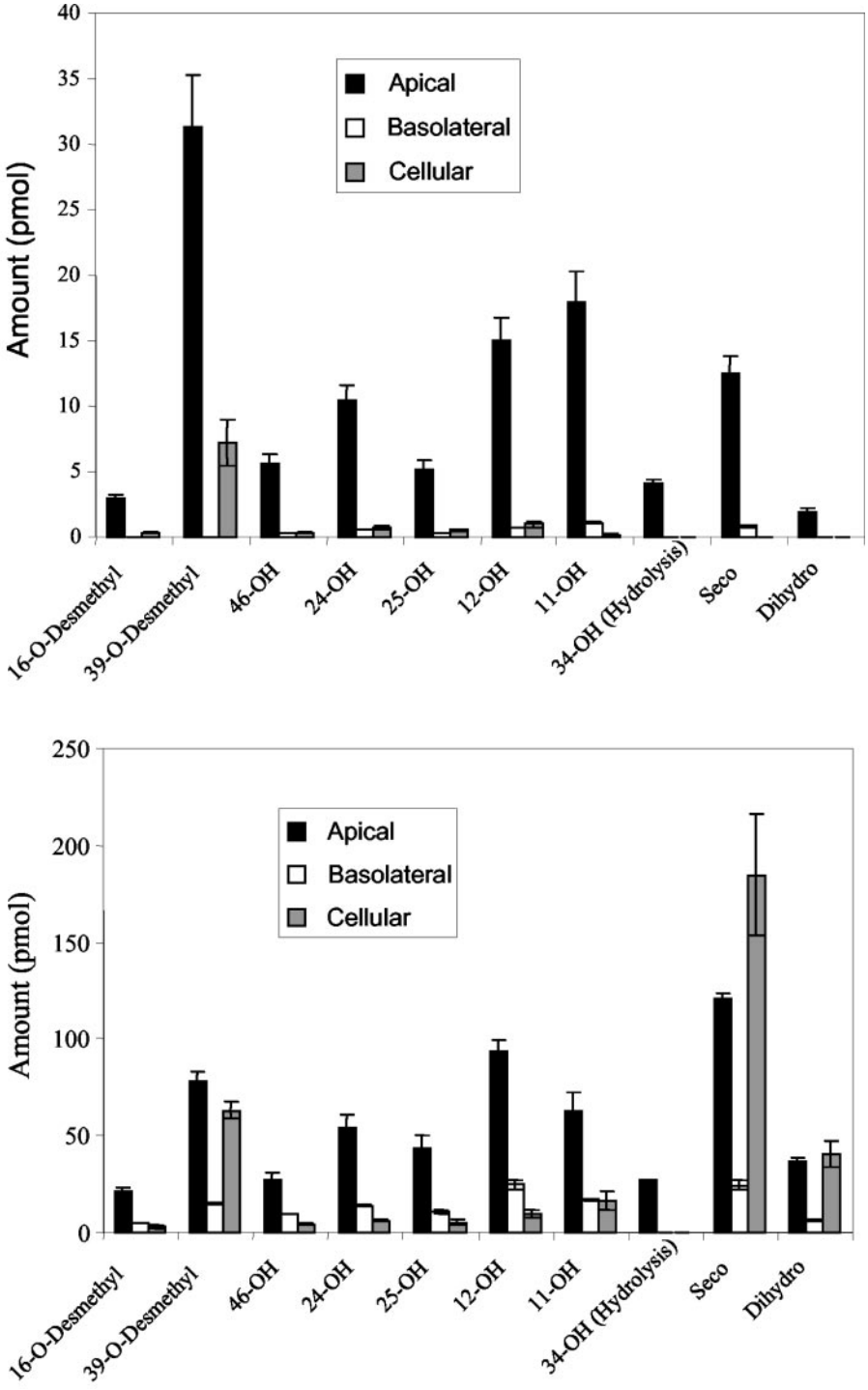

Fig. 8. Distribution of CYP3A4 metabolites and degradation products of sirolimus formed in CYP3A4-transfected Caco-2 cells 3 h after a 1 μM (top) or 20 μM (bottom) apical dose.

novel route of extraction for sirolimus in vitamin D_3-treated Caco-2 cells. The authors concluded that degradation of sirolimus to seco-sirolimus followed by metabolism of seco-sirolimus to the dihydrosirolimus could contribute significantly to first-pass metabolism in humans. Furthermore, they found very little CYP3A4-derived sirolimus metabolites after incubation with vitamin D_3-treated Caco-2 cells. They reported that most of the parent drug was degraded to the hydrolysis product (34-OH) or the ring opened isomer of sirolimus (seco-sirolimus), which was subsequently metabolized by an unknown cytosolic enzyme to the dihydrosirolimus metabolite. We believe that the vitamin D_3-induced Caco-2 cells do not contain sufficient CYP3A4 to make appropriate conclusions as to the importance of this enzyme in limiting drug absorption. The CYP3A4-transfected Caco-2 cells have been shown to have 2.5-fold higher CYP3A4 activity than vitamin D_3-treated Caco-2 cells (Cummins et al., 2001). In CYP3A4-transfected Caco-2 cells, the degradation product seco-sirolimus and its dihydro metabolite were readily observed after a 20 μM sirolimus incubation. However, the formation of seco-sirolimus seemed to be greatest on the dosing side, regardless of the direction of transport, in-

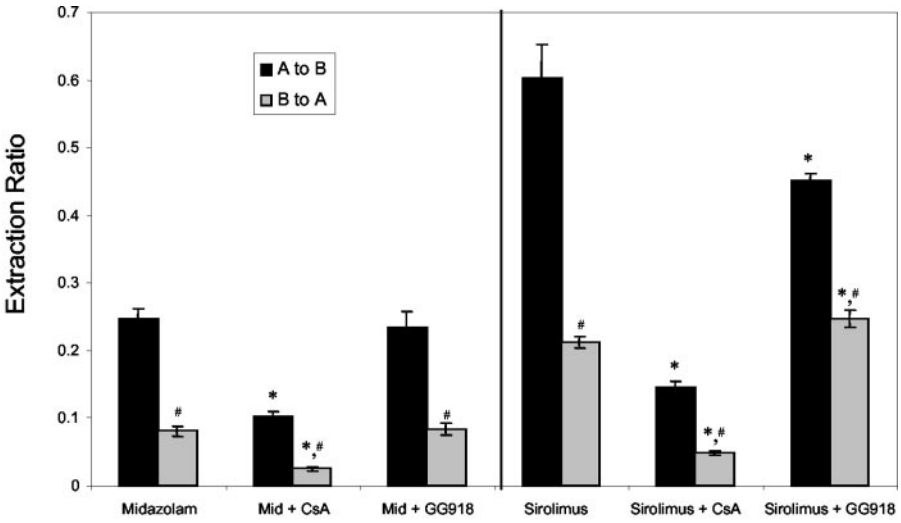

Fig. 9. Extraction ratios of midazolam and sirolimus after an apical or basolateral dose calculated using eq. 1. The effect of inhibiting P-gp on the ER is elucidated by incubation with GG918, whereas the dual effect of inhibiting CYP3A4 and P-gp on the ER is found by incubation with CsA. Data are presented as the mean ± S.D. (n = 3). *, significantly different from control for that direction (A to B and B to A) and compound (midazolam or sirolimus), $p < 0.05$. #, significantly different from A to B for that condition (control, with CsA or with GG918) for that compound, $p < 0.05$.

dicating that it was likely being formed through nonspecific degradation within the transport buffer. Because sirolimus is unstable in plasma (Streit et al., 1996), the presence of 1% FBS in our transport media (added to prevent nonspecific binding of drug to the transport equipment) may be contributing to sirolimus degradation. It is not surprising, therefore, that the fraction of seco-sirolimus increased linearly with concentration, whereas CYP3A4 metabolites did not. The total seco-sirolimus formed 3 h after an apical dose of 1 and 20 μM sirolimus was 13 and 330 pmol, respectively, whereas the CYP3A4 metabolites formed under similar conditions were 105 and 603 pmol, respectively. CYP3A4 was most likely saturated at the 20 μM concentration because the K_m for each of the sirolimus metabolites is between 1 and 2 μM (W. Jacobsen, unpublished data). Furthermore, we observed only minor amounts of the hydrolysis product of sirolimus in our incubations (we estimate that it amounts to 25% of the 39-*O*-desmethyl observed). The hydrolysis product of sirolimus (34-OH) can be formed in the presence of acid or base (Wang et al., 1994) as well as at high temperatures. It is possible that the extensive formation of the degradation products seen by Paine et al. (2002) was a result of differences in sample handling. Our samples underwent minimal sample processing as we performed on-line solid phase extraction, whereas Paine et al. (2002) performed manual extraction followed by evaporation. The higher dihydro formation observed by Paine et al. (2002) in vitamin D_3-treated Caco-2 cells may be due to the initial amount of seco-sirolimus present in the dosing solution. At time 0, approximately 13% of the radioactivity could be attributed to seco-sirolimus [estimated from Paine et al. (2002)], whereas only 1% of the dose was converted to seco-sirolimus, even after 3 h in the CYP3A4-Caco-2 cells studied here. Although evidence is lacking for the formation of seco-sirolimus in vivo, if the intestinal concentration of sirolimus is high enough to saturate CYP3A4 the contribution of the degradation pathway could be significant. The concentration of sirolimus in the gut has been estimated to be between 1.5 and 50 μM (Lampen et al., 1998).

Despite the differences between the in vitro models, several lines of evidence have suggested that intestinal CYP3A4 is important in the first-pass disposition of sirolimus. Extensive sirolimus CYP3A metabolites were observed across excised pig jejunum in Ussing chamber studies (Lampen et al., 1998) and across rat intestine after mesenteric cannulation (Crowe et al., 1999). Furthermore, coadministration of oral cyclosporine with oral sirolimus in healthy volunteers resulted in a 6-fold increase in the C_{max} and a 2.5-fold increase in the area under the concentration verus time curve for sirolimus (Rapamune product information; Wyeth-Ayerst). A similar study performed in stable kidney transplant patients found that the C_{max} was significantly increased and the T_{max} was reduced when cyclosporine was given concomitantly with sirolimus compared with cyclosporine dosing 4 h after the sirolimus dose (Kaplan et al., 1998). This interaction was most likely due to altered bioavailability because a change in T_{max} was observed and the increase in C_{max} was much greater than the change in the sirolimus trough levels. The limited role for P-gp in sirolimus absorption was recently confirmed in vivo when rats given oral sirolimus alone or in combination with D-α-tocopheryl poly(ethylene glycol 1000) succinate (an inhibitor of P-gp) showed no changes in sirolimus pharmacokinetics (Wacher et al., 2002).

The data obtained with sirolimus from CYP3A4-transfected Caco-2 cells support our previous findings with the cysteine protease inhibitor K77 that showed P-gp could increase presystemic metabolism of drugs by CYP3A4 by repeated cycling of the drug at the apical membrane (Cummins et al., 2002). These data also highlight factors that complicate our understanding of the interplay of metabolism and transport. For sirolimus, it seemed as though multiple transporters were involved and therefore the net effect of P-gp on metabolism was not as great as expected for a good P-gp substrate. Furthermore, the phenomenon of slowed permeation of midazolam from the basolateral side of the cell resulted in an approximation of the ER that was directionally dependent. The inhibition studies of sirolimus and cyclosporine in CYP3A4-transfected cells would have predicted the drug-drug interaction observed in vivo, emphasizing the utility of these cells for determining the relevant intestinal absorption barriers for a given substrate.

References

Ambudkar SV, Dey S, Hrycyna CA, Ramachandra M, Pastan I, and Gottesman MM (1999) Biochemical, cellular and pharmacological aspects of the multidrug transporter. *Annu Rev Pharmacol Toxicol* **39:**361–398.

Arceci RJ, Stieglitz K, and Bierer BE (1992) Immunosuppressants FK506 and

rapamycin function as reversal agents of the multidrug resistance phenotype. *Blood* **80:**1528–1536.
Artursson P and Borchardt RT (1997) Intestinal drug absorption and metabolism in cell cultures: Caco-2 and beyond. *Pharm Res (NY)* **14:**1655–1658.
Artursson P and Karlsson J (1991) Correlation between oral drug absorption in humans and apparent drug permeability coefficients in human intestinal epithelial (Caco-2) cells. *Biochem Biophys Res Commun* **175:**880–885.
Benet LZ, Kroetz DL, and Sheiner LB (1996a) The dynamics of drug absorption, distribution and elimination., in *Goodman & Gilman's The Pharmacological Basis of Therapeutics* (Hardman JG, Limbird LE, Molinoff PB, Ruddon RW, and Gilman AG eds) pp 3–28, McGraw-Hill Companies, New York.
Benet LZ, Wu CY, Hebert MF, and Wacher VJ (1996b) Intestinal drug metabolism and antitransport processes: a potential paradigm shift in oral drug delivery. *J Control Release* **39:**139–143.
Christians U, Jacobsen W, Serkova N, Benet LZ, Vidal C, Sewing KF, Manns MP, and Kirchner GI (2000) Automated, fast and sensitive quantification of drugs in blood by liquid chromatography-mass spectrometry with on-line extraction: immunosuppressants. *J Chromatogr B Biomed Sci Appl* **748:**41–53.
Crowe A, Bruelisauer A, Duerr L, Guntz P, and Lemaire M (1999) Absorption and intestinal metabolism of SDZ-RAD and rapamycin in rats. *Drug Metab Dispos* **27:**627–632.
Crowe A and Lemaire M (1998) In vitro and in situ absorption of SDZ-RAD using a human intestinal cell line (Caco-2) and a single pass perfusion model in rats: comparison with rapamycin. *Pharm Res (NY)* **15:**1666–1672.
Cummins CL, Jacobsen W, and Benet LZ (2002) Unmasking the dynamic interplay between intestinal P-glycoprotein and CYP3A4. *J Pharmacol Exp Ther* **300:**1036–1045.
Cummins CL, Mangravite LM and Benet LZ (2001) Characterizing the expression of CYP3A4 and efflux transporters (P-gp, MRP1 and MRP2) in CYP3A4-transfected Caco-2 cells after induction with sodium butyrate and the phorbol ester 12-O-tetradecanoylphorbol-13-acetate. *Pharm Res (NY)* **18:**1102–1109.
Dias VC and Yatscoff RW (1994) Investigation of rapamycin transport and uptake across absorptive human intestinal cell monolayers. *Clin Biochem* **27:**31–36.
Fisher JM, Wrighton SA, Watkins PB, Schmiedlin-Ren P, Calamia JC, Shen DD, Kunze KL, and Thummel KE (1999) First-pass midazolam metabolism catalyzed by 1alpha,25-dihydroxy vitamin D3-modified Caco-2 cell monolayers. *J Pharmacol Exp Ther* **289:**1134–1142.
Hallensleben K, Raida M, and Habermehl G (2000) Identification of a new metabolite of macrolide immunosuppressant, like rapamycin and SDZ RAD, using high performance liquid chromatography and electrospray tandem mass spectrometry. *J Am Soc Mass Spectrom* **11:**516–525.
Jacobsen W, Serkova N, Hausen B, Morris RE, Benet LZ, and Christians U (2001) Comparison of the in vitro metabolism of the macrolide immunosuppressants sirolimus and RAD. *Transplant Proc* **33:**514–515.
Kaplan B, Meier-Kriesche HU, Napoli KL, and Kahan BD (1998) The effects of relative timing of sirolimus and cyclosporine microemulsion formulation coadministration on the pharmacokinetics of each agent. *Clin Pharmacol Ther* **63:**48–53.
Kim RB, Wandel C, Leake B, Cvetkovic M, Fromm MF, Dempsey PJ, Roden MM, Belas F, Chaudhary AK, Roden DM, et al. (1999) Interrelationship between substrates and inhibitors of human CYP3A and P-glycoprotein. *Pharm Res (NY)* **16:**408–414.
Lampen A, Zhang Y, Hackbarth I, Benet LZ, Sewing KF, and Christians U (1998) Metabolism and transport of the macrolide immunosuppressant sirolimus in the small intestine. *J Pharmacol Exp Ther* **285:**1104–1112.
Paine MF, Leung LY, Lim HK, Liao K, Oganesian A, Zhang MY, Thummel KE, and Watkins PB (2002) Identification of a novel route of extraction of sirolimus in human small intestine: roles of metabolism and secretion. *J Pharmacol Exp Ther* **301:**174–186.
Paine MF, Shen DD, Kunze KL, Perkins JD, Marsh CL, McVicar JP, Barr DM, Gillies BS, and Thummel KE (1996) First-pass metabolism of midazolam by the human intestine. *Clin Pharmacol Ther* **60:**14–24.
Polli JW, Wring SA, Humphreys JE, Huang L, Morgan JB, Webster LO, and Serabjit-Singh CS (2001) Rational use of in vitro P-glycoprotein assays in drug discovery. *J Pharmacol Exp Ther* **299:**620–628.
Schmiedlin-Ren P, Thummel KE, Fisher JM, Paine MF, Lown KS, and Watkins PB (1997) Expression of enzymatically active CYP3A4 by Caco-2 cells grown on extracellular matrix-coated permeable supports in the presence of 1alpha,25-dihydroxyvitamin D3. *Mol Pharmacol* **51:**741–754.
Streit F, Christians U, Schiebel HM, Napoli KL, Ernst L, Linck A, Kahan BD, and Sewing KF (1996) Sensitive and specific quantification of sirolimus (rapamycin) and its metabolites in blood of kidney graft recipients by HPLC/electrospray-mass spectrometry. *Clin Chem* **42:**1417–1425.
Tolle-Sander S, Rautio J, Wring S, Polli JW, and Polli JE (2003) Midazolam exhibits characteristics of a highly permeable P-glycoprotein substrate. *Pharm Res (NY)* **20:**757–764.
Wacher VJ, Silverman JA, Wong S, Tran-Tau P, Chan AO, Chai A, Yu XQ, O'Mahony D, and Ramtoola Z (2002) Sirolimus oral absorption in rats is increased by ketoconazole but is not affected by D-alpha-tocopheryl poly(ethylene glycol 1000) succinate. *J Pharmacol Exp Ther* **303:**308–313.
Wacher VJ, Wu CY, and Benet LZ (1995) Overlapping substrate specificities and tissue distribution of cytochrome P450 3A and P-glycoprotein: implications for drug delivery and activity in cancer chemotherapy. *Mol Carcinog* **13:**129–134.
Wang CP, Chan KW, Schiksnis RA, Scatina J, and Sisenwine SF (1994) High performance liquid chromatographic isolation, spectroscopic characterization and immunosuppressive activities of two rapamycin degradation products. *J Liq Chromatogr* **17:**3383–3392.
Yee S (1997) In vitro permeability across Caco-2 cells (colonic) can predict in vivo (small intestinal) absorption in man–fact or myth. *Pharm Res (NY)* **14:**763–766.

Address correspondence to: Dr. Leslie Z. Benet, Biopharmaceutical Sciences, University of California San Francisco, 533 Parnassus Ave. U-68, San Francisco, CA 94143-0446. E-mail: benet@itsa.ucsf.edu